JOURNAL OF AIRCRAFT
Vol. 44, No. 4, July–August 2007

Engineering Notes

ENGINEERING NOTES are short manuscripts describing new developments or important results of a preliminary nature. These Notes should not exceed 2500 words (where a figure or table counts as 200 words). Following informal review by the Editors, they may be published within a few months of the date of receipt. Style requirements are the same as for regular contributions (see inside back cover).

Prediction of Hovering Rotor Noise Based on Reynolds-Averaged Navier–Stokes Simulation

Wen Ping Song,* Zhong Hua Han,† and Zhi De Qiao‡
Northwestern Polytechnical University, 710072 Xi'an, People's Republic of China

DOI: 10.2514/1.28310

I. Introduction

OVER the past decade, the hybrid method [coupling computational fluid dynamics (CFD) techniques with advanced analytic methods based on acoustic analogy, such as the Ffowcs Williams–Hawkings equation with penetrable data surface (FW–H_{pds}) method] has been successfully applied to predict the complicated acoustic field of helicopter rotors.

The Ffowcs Williams–Hawkings (FW–H) equation [1], a rearrangement of Navier–Stokes equations by using general-function theory, provides an accurate theoretical model for describing the propagation of noise from a moving surface to the far field. The Farassat 1A method for solving the linear part of the FW–H equation was developed by Farassat and Succi [2]. It has been successfully applied in linear noise prediction [2,3] for more than 20 years. The Farassat 1A method predicts discrete frequency noise quite well, but it would run into complication when predicting nonlinear quadrupole noise of helicopter rotors, because the data surface is the blade itself and nonlinear effects are not included in the surface integral. To calculate the nonlinear noise [e.g., high-speed impulsive (HSI) noise], Farassat and Myers [4] derived the general form of the Kirchhoff equation and its solution (known as the Kirchhoff formulation) to describe the noise radiation from a moving surface. The data surface of the Kirchhoff formulation is fictitious and penetrable. The main benefit of the Kirchhoff method is that the nonlinear effect is accounted for by performing the integral on the data surface covering the nonlinear flow region. The Kirchhoff method coupled with the near-field CFD solution (called the CFD/Kirchhoff method) has proven to be accurate and efficient when predicting impulsive noise. More recently, a new form of FW–H equation with a penetrable surface (called the FW–H_{pds} equation) was proposed by Crighton et al. [5] to improve the efficiency of solving the quadrupole noise. The method using a penetrable data surface for solving the FW–H equation with the Euler solution as input data was first implemented by di Francescantonio [6] for prediction of far-field noise from transonic helicopter rotors in hover. Brentner and Farassat [7] conducted an analytical comparison of the FW–H_{pds} method with the Kirchhoff method and concluded that the FW–H_{pds} method is more accurate and robust than the Kirchhoff method when the data surface is located in the nonlinear flow region. The FW–H_{pds} method rapidly showed promise in the study work of a few researchers [7–10] when it was used for predicting the noise generated by helicopter rotors in hover and forward flight. More recently, Farassat and Casper [11] emphasized the role of analytical methods in computational aeroacoustics and recommended FW–H_{pds} as a very promising method for noise prediction of a complicated flowfield.

To predict nonlinear noise generated by transonic rotors in hover, three-dimensional Euler equations were commonly used to consider the nonlinear effect related to shock waves. To consider the influence of viscous effect in the near field and get more accurate information about noise sources, this paper uses Reynolds-Averaged Navier–Stokes (RANS) equations to model the nonlinear viscous flowfield near the rotor blades. The far-field noise is calculated by a retarded-time integral formula solving the FW–H_{pds} equation, with the solution of the RANS equations taken as input data.

II. RANS Method for a Transonic Helicopter Rotor in Hover

Simulation of quasi-steady flow over helicopter rotors in hover uses a relative coordinate system fixed on a rotor blade. The grids around a single blade are generated (see Figs. 1 and 2) and the flowfield around only a single rotor blade is simulated. The influence of other blades is accounted for by performing a periodic boundary condition. Chimera-grid methodology is used to effectively capture the viscous effect near a rotor blade and implement the periodic boundary condition.

Three-dimensional unsteady RANS equations in a relative coordinate system fixed on a rotor blade can be written as

$$\iiint_V \frac{\partial \boldsymbol{W}}{\partial t}\,\mathrm{d}V + \iint_S (\overline{\overline{\boldsymbol{F}}} - \overline{\overline{\boldsymbol{F}}}_v)\cdot \boldsymbol{n}\,\mathrm{d}S + \iiint_V \boldsymbol{G}\,\mathrm{d}V = 0 \qquad (1)$$

where V is the control volume, and S and $\boldsymbol{n}$ denote the boundary of the control volume and its unit normal outer vector, respectively. The expressions of flow variable vector, inviscid flux vector, and viscous flux vector are omitted here and can be referred to in [12]. For turbulent flow, the Baldwin–Lomax [13] algebraic turbulence model is used for all of the calculation in the present work. The governing equations are solved by a finite volume method developed by Jameson et al. [14].

III. Acoustic Method Based on the FW–H_{pds} Equation

A. FW–H_{pds} Equation and Solution

The FW–H equation was taken as the most general form of the Lighthill acoustic analogy.

In 1969, Ffowcs Williams and Hawkings [1] rearranged the Navier–Stokes equation in fluid dynamics by applying general-

Received 12 October 2006; revision received 15 February 2007; accepted for publication 25 February 2007.

*Professor, National Key Laboratory of Aerodynamic Design and Research, School of Aeronautics, P.O. Box 754, 127 West Youyi Road; wpsong@nwpu.edu.cn.

†Doctoral Candidate, National Key Laboratory of Aerodynamic Design and Research, School of Aeronautics, P.O. Box 754, 127 West Youyi Road; hanzh@nwpu.edu.cn.

‡Professor, National Key Laboratory of Aerodynamic Design and Research, School of Aeronautics, P.O. Box 754, 127 West Youyi Road; zdqiao@nwpu.edu.cn.

function theory and obtained an inhomogeneous wave equation (namely, the well-known FW–H equations) that can give the exact governing equation of an acoustic field generated by a wall boundary in arbitrary motion. Consider a piecewise smooth surface defined by $f(\mathbf{x}, t) = 0$, which surrounds a rotor blade or other types of wall boundaries moving in a stationary fluid. Assuming that $\nabla f = \boldsymbol{n}$ and $\partial f/\partial t = -v_n$ ($\boldsymbol{n}$ denotes the unit normal outer vector, $\boldsymbol{v}$ is the velocity vector of the control surface, and $\boldsymbol{v} \cdot \boldsymbol{n} = v_n$), then the FW–H equation can be written as

$$\left(\frac{1}{c^2}\frac{\partial^2}{\partial t^2} - \frac{\partial^2}{\partial x_i^2}\right) p'(x_i, t) = \frac{\bar{\partial}}{\partial t}\{[(\rho_0 v_n + \rho(u_n - v_n)]\delta(f)\} - \frac{\bar{\partial}}{\partial x_i}\{[-P'_{ij} \cdot n_j + \rho u_i(u_n - v_n)]\delta(f)\} + \frac{\bar{\partial}^2}{\partial x_i x_j}[T_{ij}H(f)] \quad (2)$$

Where, c, ρ, u_i, and P_{ij} denote the speed of sound, density, tensors of velocity, and stress, respectively; $p'$is acoustic pressure; $T_{ij} = -P'_{ij} + \rho u_i u_j - c^2\rho'\delta_{ij}$ is the Lighthill stress tensor; δ_{ij} is the Kronecker delta; subscript 0 indicates the freestream undisturbed quantities; superscript prime denotes the disturbed values; $H(f)$ is the Heaviside function, and $\delta(f)$ is the Dirac function, which satisfies

$$H(f) = \begin{cases} 1 & f(x_i, t) > 0 \\ 0 & f(x_i, t) < 0 \end{cases}$$

and

$$\delta(f) = \frac{\bar{\partial} H(f)}{\partial f}$$

Using a penetrable data surface $f(x_i, t) = 0$, including the entire acoustic source, the retarded-time solution of Eq. (2) for a penetrable data surface can be obtained directly, according to the Farassat 1A formula. The retarded-time integration solution of the FW–H_{pds} equation according to the Farassat 1A formula can been found in [7] and will not be listed here.

B. Choices of Data Surface and Solution of the Retarded-Time Equation

To perform the integral on the data surface, two key points should be highlighted in this paper. They are 1) choices of data surface and 2) solution of the retarded-time equation.

To perform the integration of the time-domain integral method (such as Formula 1A), the first key point is the appropriate choice of data surface. There are two types of data surfaces that are generally used in rotor-noise prediction (namely, rotating data surface and nonrotating data surface), and both are used in this study. The rotating surface is selected because some surfaces of the CFD grid that have the same angular velocity of the rotors. The main advantage of using the rotating surface is in that the aerodynamic data on the data surface can be directly obtained from CFD solutions; hence, the numerical interpolation is avoided. The nonrotating data surface is defined as a cylindrical surface that is relatively stationary with respect to the blade hub. The advantage of the nonrotating surface is that with it, the retarded time can be solved explicitly, as will be shown in the following formula (3). The nonrotating surface is divided into elements along its axial and circular directions. To quickly obtain the aerodynamic data of these elements, a 3-D linear interpolation is performed from the CFD solution. A fast-searching-methodology-based inverse map is used to improved the efficiency of searching the contribution CFD grid cell for a considering point.

As stated in [15], some of the quadrupole sources lie outside the sonic circle when the delocalization of the shock system occurs at a high tip-Mach number. In this case, the integration surface should be placed outside the sonic circle and extended far away from the rotor tip. Then the rotating data surface cannot be used, because the speed of the data surface will be larger than the sonic speed and the Farassat 1A method will break down. For the supersonic rotation surface, an alternate solution of the FW–H_{pds} equation based on the collapsed-sphere method should be employed (it will not be discussed here). In this paper, when delocalization of the shock system occurs, the nonrotation surface is used and the Farassat 1A method mentioned earlier still works well.

Another key point is the solution of the retarded-time equation. For the noise prediction of helicopter rotors in hover, the retarded-time equation can be written as

$$\tau = t - \frac{1}{c_0}\left|\boldsymbol{x}_0 - \begin{bmatrix} \cos(\omega_s\tau) & 0 & -\sin(\omega_s\tau) \\ 0 & 1 & 0 \\ \sin(\omega_s\tau) & 0 & \cos(\omega_s\tau) \end{bmatrix}\boldsymbol{y}_0\right| \quad (3)$$

where τ is the retarded time for a given observing point; $\boldsymbol{x}_0$and $\boldsymbol{y}_0$ denote the coordinate vectors of the observing and the source point at zero time, respectively; ω_s is the angular velocity of the rotating data surface, which is chosen to be the same value as the angular velocity of the rotors. Note that $\omega_s = 0$ corresponds to the nonrotating data surface. For $\omega_s = 0$, Eq. (3) is an explicit formula for τ. However, the solution of this equation cannot be explicitly deduced if $\omega_s \neq 0$. In this paper, a solution method based on a simple iteration technique is developed for the rotating data surface, and a good convergence is achieved.

IV. Results and Discussion

All simulations in this section are performed using a rotor grid of the C-H type with a grid number of $169 \times 49 \times 65$ and a background grid of the H-H type with a grid number of $101 \times 81 \times 91$ (as illustrated in Figs. 1 and 2). The rotor grids have the first near-surface grid point below $y+ = 0.7$, to ensure that the sublayer of the turbulent shear flow is sufficiently resolved. The definition of the Reynolds number is based on the chord and the tip-Mach number of the rotor blade.

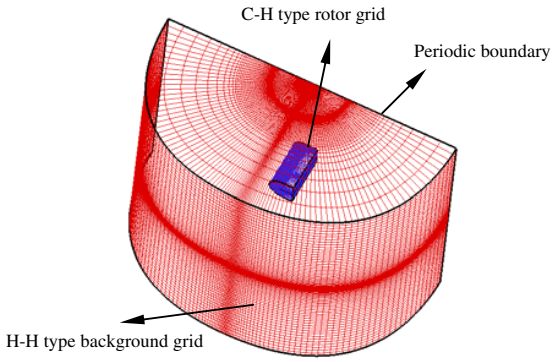

Fig. 1 Schematics of the chimera grid for a single rotor blade.

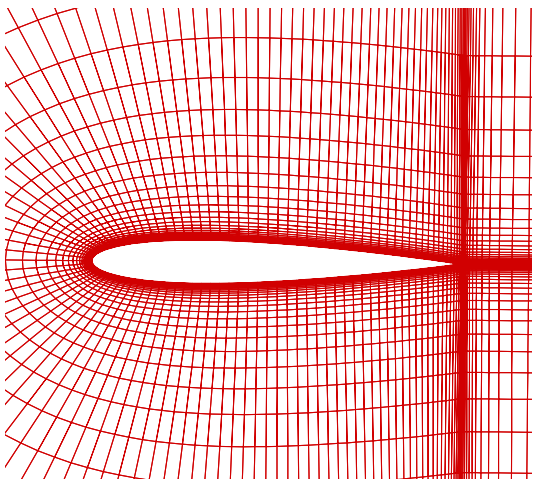

Fig. 2 Schematics of one section of the rotor grid.

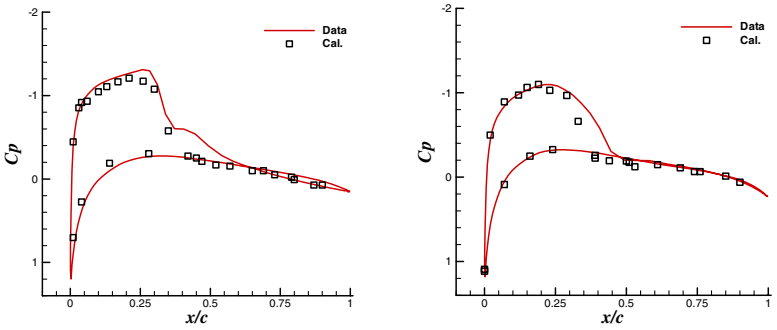

a) r/R=0.89 b) r/R=0.96

Fig. 3 Comparison of the computed pressure distribution and experimental data.

A. Validation of the RANS Flow Solver

The simulation of flow over a Caradonna and Tung [16] rotor is performed to validate the RANS flow solver.

The validation case is the transonic lifting rotor with a tip-Mach number of 0.877, a Reynolds number of 3.93×10^6, and a collective pitch angle of 8 deg. The comparison of computed pressure distribution and experimental data for two different locations ($r/R = 0.89$ and $r/R = 0.96$) is demonstrated in Figs. 3a and 3b, and the agreement is very good. It is also shown that the shock wave that occurs in the flowfield near the blade tip is correctly captured.

B. Validation of the RANS/FW–H_{pds} Method

To validate the present RANS/FW–H_{pds} method for HSI noise of transonic rotors, a UH-1H model is adopted. The experimental data were published by Boxwell et al. in [17]. The observing microphone is located $R = 3.09$ away from the rotation axis (R is the radius of the rotor).

The near field of the UH-1H rotor is simulated by the RANS method presented in Sec. II. The rotating data surface consists of some of the grid surfaces of the C-H type of rotor grid (see Fig. 4), and the flow variables on the data surface are calculated directly from the RANS solution on a rotor grid; the nonrotational data surface is constructed as a circular cylinder (see Fig. 5). The cylinder is divided as 1440×30 surface elements (1440 segments along the circular direction and 30 segments along the axial direction). The value of flow variables on the cylinder is obtained by a 3-D linear interpolation from the flowfield on the background grid.

Figure 6 shows the comparison of predicted acoustic pressure and experiment data at a tip-Mach number of 0.85. A nonrotating circular cylinder with a radius of $R = 1.2$ is used as the data surface. The computed results show good agreement with experimental data. Figure 7 shows the comparison of predicted acoustic pressure in one period using rotating and nonrotating data surfaces, and little difference was found. One can conclude that by the RANS/FW–H_{pds} method, both rotating and nonrotating data surfaces are nearly identically adequate for predicting the nonlinear noise of transonic rotors. The average time for predicting a single observing point is about 1 min on a Pentium IV 3.4 GHz personal computer, which indicates that the present method is very efficient.

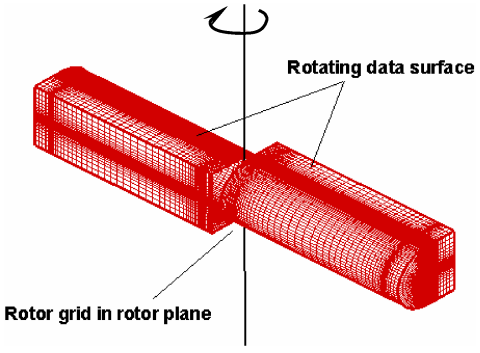

Fig. 4 Schematics of the rotating data surface.

C. Comparison of Different Acoustic Methods

The present RANS/FW–H_{pds} method is compared with the Euler/FW–H_{pds} method and the Farassat 1A method. Prediction of the HSI noise of the UH-1H rotor described in Sec. IV.B is performed.

Figure 8 shows the predicted acoustic pressure versus time for a tip-Mach number of 0.90 and Reynolds number of 1.6×10^6. The observing point is located at an in-rotor-plane point that is $R = 3.09$ away from the rotation axis. Figure 9 shows the predicted acoustic pressure versus time for a tip-Mach number of 0.88 and Reynolds number of 1.56×10^6. The observing point is located at an in-rotor-plane point that is $R = 1.78$ away from the rotation axis.

In Figs. 8 and 9, the results of the Farassat 1A method are linear noise, including thickness and loading noise. Compared with the Farassat 1A method, the RANS/FW–H_{pds} method and the Euler/FW–H_{pds} method can predict nonlinear noise, which is clearly demonstrated in Figs. 8 and 9. The negative-acoustic-pressure peak calculated by using the RANS/FW–H_{pds} method is higher and more consistent with the experimental data compared with that calculated by the Euler/FW-H_{pds} method. The reason can be explained as being that the nonlinear noise due to viscous effect and downwash of the wake system is taken into account more accurately when using a solution of Navier–Stokes equations as input data.

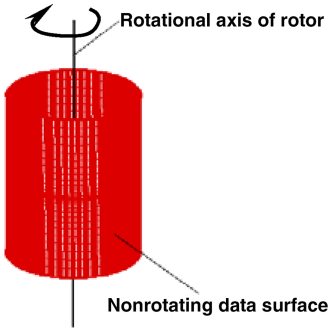

Fig. 5 Schematics of the nonrotating data surface.

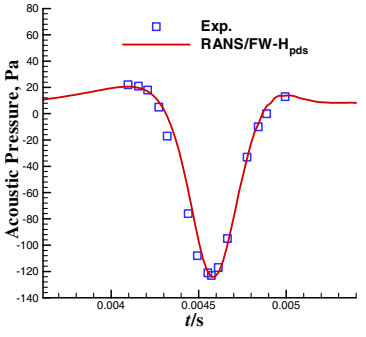

Fig. 6 Comparison of predicted acoustic pressure and experimental data ($Ma_{tip} = 0.85$).

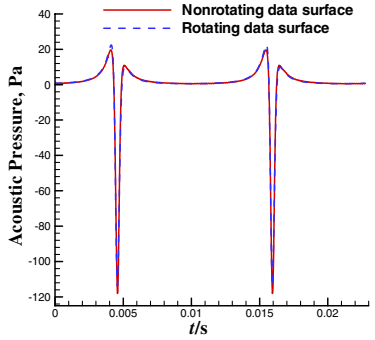

Fig. 7 Comparison of predicted acoustic pressure in one period using rotating and nonrotating data surfaces ($Ma_{tip} = 0.85$).

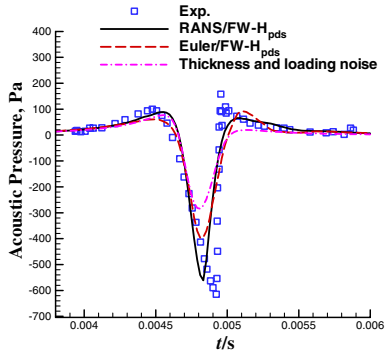

Fig. 8 Comparison of acoustic pressure signatures predicted by different acoustic methods ($Ma_{tip} = 0.90$) with measurements.

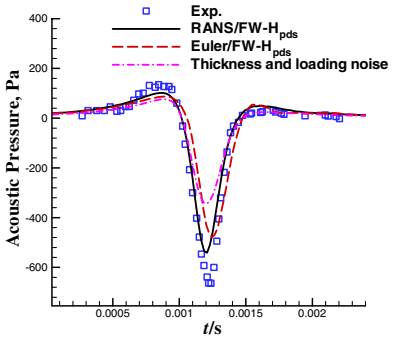

Fig. 9 Comparison of acoustic pressure signatures predicted by different acoustic methods ($Ma_{tip} = 0.88$) with measurements.

V. Conclusions

A computational aeroacoustic method combining the RANS simulation with the FW–H$_{pds}$ method is presented and studied. The results of RANS simulation using chimera-grid methodology is validated for the Caradonna and Tung [16] rotor model. The computed acoustic pressure using RANS/FW–H$_{pds}$ for the UH-1H rotor is compared with experimental data and shows good agreement. Comparison of RANS/FW–H$_{pds}$ and Euler/FW–H$_{pds}$ predictions with measurements shows that the acoustic prediction using the RANS/FW–H$_{pds}$ method is more accurate, due to the capture of viscous effect and wake systems in the flow over the rotor blades.

Acknowledgments

Wen Ping Song thanks Ai Ming Yang for sharing his technical material and experience in rotor flow simulations and for many useful technical discussions.

References

[1] Ffowcs Williams, J. E., and Hawkings, D. L., "Sound Generated by Turbulence and Surfaces in Arbitrary Motion," *Philosophical Transactions of the Royal Society of London, Series A: Mathematical and Physical Sciences*, Vol. A264, No. 1151, 1969, pp. 321–342.

[2] Farassat, F., and Succi, G. P., "A Review of Propeller Discrete Frequency Noise Prediction Technology with Emphasis on Two Current Methods for Time Domain Calculations," *Journal of Sound and Vibration*, Vol. 71, No. 3, 1980, pp. 399–419.

[3] Kenneth, K. B., "Prediction of Helicopter Discrete Frequency Rotor Noise—A Computer Program Incorporating Realistic Blade Motions and Advanced Formulation," NASA TM 87721, Oct. 1986.

[4] Farassat, F., and Myers, M. K., "Extension of Kirchhoff's Formulation to Radiation from Moving Surface," *Journal of Sound and Vibration*, Vol. 23, No. 3, 1988, pp. 451–460.

[5] Crighton, D. G., Dowling, A. P., Ffowcs Williams, J. E., Heckl, M., and Leppington, F. G., *Modern Method in Analytical Acoustics: Lecture Notes*, Springer–Verlag, London, 1992.

[6] Di Francescantonio, P., "A New Boundary Integral Formulation for the Prediction of Sound Radiation," *Journal of Sound and Vibration*, Vol. 202, No. 4, 1997, pp. 191–509.

[7] Brentner, K. S., and Farassat, F., "Analytical Comparison of the Acoustic Analogy and Kirchhoff Formulation for Moving Surfaces," *AIAA Journal*, Vol. 36, No. 8, 1998, pp. 1379–1386.

[8] Brentner, K. S., "Modeling Aerodynamically Generated Sound: Recent Advance in Rotor Noise Prediction," AIAA Paper 2000-0345, 2000.

[9] Lockard, D., "A Comparison of Ffowcs Williams-Hawkings Solvers for Airframe Noise Applications," AIAA Paper 2002-2580, June 2002.

[10] Han, Z. H., Song, W. P., and Qiao, Z. D., "Investigation of Rotor Noise Prediction Using Different Aeroacoustic Methods in Time Domain," 24th International Congress of the Aeronautical Sciences, Yokohama, Japan, International Congress of the Aeronautical Sciences Paper 2004-3.4.R, 2004.

[11] Farassat , F., and Casper, J. H., "Towards an Airframe Noise Prediction Methodology: Survey of Current Approaches," AIAA Paper 2006-0210, Jan. 2006.

[12] Yang, A. M., and Qiao., Z. D., "A New Way of Simulating the flowfield of a Lifting Rotor in Hover," *Journal of Northwestern Polytechnical University*, Vol. 18, No. 4, 2000, pp. 579–582.

[13] Baldwin, B., and Lomax, H., "Thin Layer Approximation and Algebraic Model for Separated Turbulent Flow," AIAA Paper 1978-257, 1978.

[14] Jameson, A., Schmidt, W., and Turkel, E., "Numerical Solutions of the Euler Equations by a Finite Volume Method Using Runge-Kutta Time Stepping Schemes," AIAA Paper 1981-1259, 1981.

[15] Farassat, F., and Brentner, K. S., "Supersonic Quadrupole Noise Theory for High-Speed Helicopter Rotors," *Journal of Sound and Vibration*, Vol. 218, No. 3, 1998, pp. 481–500.

[16] Caradonna, F. X., and Tung, C., "Experimental and Analytical Studies of a Model Helicopter Rotor in Hover," NASA TM 81232, 1981.

[17] Boxwell, D. A., Yu, Y. H., and Schmitz, F. H., "Hovering Impulsive Noise: Some Measured and Calculated Results," *Vertica*, Vol. 3, No. 1, 1979, pp. 35–45.